BMC Biochemistry

Research article

Calmodulin binding to recombinant myosin-1c and myosin-1c IQ peptides

Peter G Gillespie*[1] and Janet L Cyr[1,2]

Address: [1]Oregon Hearing Research Center and Vollum Institute, Oregon Health & Science University, Portland OR 97239, USA and [2]Present address: Department of Otolaryngology & Sensory Neuroscience Research Center, West Virginia University School of Medicine, Morgantown WV 26506, USA

E-mail: Peter G Gillespie* - gillespp@ohsu.edu; Janet L Cyr - jcyr@hsc.wvu.edu

*Corresponding author

Published: 26 November 2002

BMC Biochemistry 2002, **3**:31

Received: 22 August 2002
Accepted: 26 November 2002

This article is available from: http://www.biomedcentral.com/1471-2091/3/31

Abstract

Background: Bullfrog myosin-1c contains three previously recognized calmodulin-binding IQ domains (IQ1, IQ2, and IQ3) in its neck region; we identified a fourth IQ domain (IQ4), located immediately adjacent to IQ3. How calmodulin binds to these IQ domains is the subject of this report.

Results: In the presence of EGTA, calmodulin bound to synthetic peptides corresponding to IQ1, IQ2, and IQ3 with K_d values of 2–4 μM at normal ionic strength; the interaction with an IQ4 peptide was much weaker. Ca^{2+} substantially weakened the calmodulin-peptide affinity for all of the IQ peptides except IQ3. To reveal how calmodulin bound to the linearly arranged IQ domains of the myosin-1c neck, we used hydrodynamic measurements to determine the stoichiometry of complexes of calmodulin and myosin-1c. Purified myosin-1c and T701-Myo1c (a myosin-1c fragment with all four IQ domains and the C-terminal tail) each bound 2–3 calmodulin molecules. At a physiologically relevant temperature (25°C) and under low-Ca^{2+} conditions, T701-Myo1c bound two calmodulins in the absence and three calmodulins in the presence of 5 μM free calmodulin. Ca^{2+} dissociated nearly all calmodulins from T701-Myo1c at 25°C; one calmodulin was retained if 5 μM free calmodulin was present.

Conclusions: We inferred from these data that at 25°C and normal cellular concentrations of calmodulin, calmodulin is bound to IQ1, IQ2, and IQ3 of myosin-1c when Ca^{2+} is low. The calmodulin bound to one of these IQ domains, probably IQ2, is only weakly associated. Upon Ca^{2+} elevation, all calmodulin except that bound to IQ3 should dissociate.

Background

Myosin-1c (Myo1c), the myosin previously called myosin-Iβ, myr 2, or MI-110K [1], is an unconventional myosin isozyme implicated in nuclear transcription [2], lamellopodia dynamics of motile cells [3,4], brush-border dynamics of proximal-tubule cells of the kidney [5,6], and adaptation of mechanoelectrical transduction in hair cells, the sensory cells of the inner ear [7]. Myo1c belongs to the myosin-I class, which contains eight members in humans [8] and mice [9]; the bullfrog genome possesses at least two members [10]. Members of the myosin-I class have a single globular motor domain, followed by a neck

region and a relatively short (30–40 kD) tail domain (Fig. 1A). This latter domain is highly basic and binds to acidic phospholipids [11]. Like all biochemically characterized unconventional myosins, Myo1c binds calmodulin light chains in its neck region [12]; this region also interacts with non-calmodulin receptors in hair cells [13].

Unconventional myosins contain from one to several IQ domains, which are calmodulin-binding motifs that adhere to the general consensus sequence IQX_3RGX_3R [14]. Calmodulin, which can bind up to four Ca^{2+} ions, generally binds IQ domains in the Ca^{2+}-free conformation; interaction of Ca^{2+}-bound calmodulin to other proteins occurs through alternative binding motifs [14].

Myo1c contains three readily recognized IQ motifs of 23 amino acids each (Fig. 1C; refs. [10,15–18]). Purified Myo1c apparently includes 2–3 calmodulins per Myo1c heavy chain [19–21]; calmodulin supplementation can increase the stoichiometry to as many as 4 calmodulins per Myo1c [21]. Unfortunately, the lack of appropriate quantitation standards for the Myo1c heavy chain in those experiments limits the reliability of these values.

How Ca^{2+} and calmodulin regulate Myo1c or indeed any myosin-I is unclear. Although Ca^{2+} increases ATPase activity of most myosin-I isozymes, *in vitro* motility is usually blocked under identical conditions [11]. Ca^{2+} dissociates one or more calmodulins from the myosin-calmodulin complex, which apparently elevates ATPase activity and inhibits motility [11]. In conventional myosin, light chains related to calmodulin appear to be essential for stabilization of the myosin lever arm [22], a domain that is vital for efficient conversion of chemical energy into mechanical work [23]. Calmodulin probably plays a similar lever-arm stabilizing role for Myo1c; Ca^{2+}-induced calmodulin release would reverse the stabilization and inhibit motility.

To better understand the regulation of Myo1c activity by calmodulin, we sought to more accurately determine how calmodulin binds to Myo1c by measuring the Ca^{2+}-dependence of calmodulin binding to individual Myo1c IQ peptides. In addition, to examine the consequences of calmodulin binding to adjacent IQ domains, we measured hydrodynamic properties of recombinant Myo1c-calmodulin complexes, under differing conditions of Ca^{2+}, calmodulin, and temperature. These measurements allowed us to determine the molecular mass and hence stoichiometry of the Myo1c complex. Our results indicate that IQ1, IQ2, and IQ3 have calmodulin bound when the concentration of Ca^{2+} is low, and that increased Ca^{2+} induces release of calmodulin from IQ1 and IQ2.

Results

Sequence analysis of IQ domains

Examination of the primary sequence of the bullfrog Myo1c neck region reveals an exact repeat of five amino acids located both in the IQ3 region (YRNQP; residues 761–765) and at residues 786–790. Alignment of the residues surrounding the repeat revealed reasonable homology with the three known IQ domains, with particular similarity to IQ3, suggesting that this region may be a fourth IQ domain (Fig. 1C). Although the pair of amino acids (LM; residues 782 and 783) that align with the RG of the IQ consensus motif are not conserved, the first pair of amino acids (IR; residues 777 and 778) that align with the consensus IQ adhere to the consensus better than those of IQ3. Because of the sequence similarity to IQ3 and because this peptide binds calmodulin (albeit weakly; see below), we refer to this domain as IQ4.

IQ – Alexa-calmodulin interaction on plastic plates

To investigate the calmodulin-binding properties of each Myo1c IQ domain, we measured interaction of a fluorescently labeled calmodulin (Alexa-calmodulin) with individual Myo1c IQ peptides that had been conjugated to wells of a plastic plate. We used an IQ peptide from neuromodulin [24] as a positive control; calmodulin binds to this site, with its interaction reduced by high ionic strength [24,25]. As a negative control, we used a peptide (PVP), corresponding to the 25 amino acids of Myo1c immediately following IQ4. Indeed, Alexa-calmodulin bound to wells derivatized with the neuromodulin IQ peptide and did not bind to the PVP peptide (Fig. 2A).

Substantial amounts of Alexa-calmodulin bound to wells derivatized with IQ1, IQ2, and IQ3; by contrast, relatively little bound to IQ4-coated wells under these conditions (Fig. 2A). As has been noted for the neuromodulin IQ domain [25], increasing the KCl concentration reduced binding to each IQ peptide. Although the data shown in Fig. 2A were obtained at room temperature, we saw a similar rank order of binding – albeit with lower total Alexa-calmodulin bound – at 4°C (data not shown).

To confirm the approximate binding strength reported by this assay, we used free IQ peptides to prevent Alexa-calmodulin binding to an IQ3-derivatized plate. Because the IQ peptides strongly quenched Alexa-calmodulin fluorescence when bound, we corrected fluorescence measurements using an identical assay in an underivatized plate. Although this quenching correction introduced substantial scatter into the data, we found that the apparent affinities for binding of peptides to Alexa-calmodulin followed the order IQ3 > IQ1 ≈ IQ2 > IQ4 (Fig. 2B).

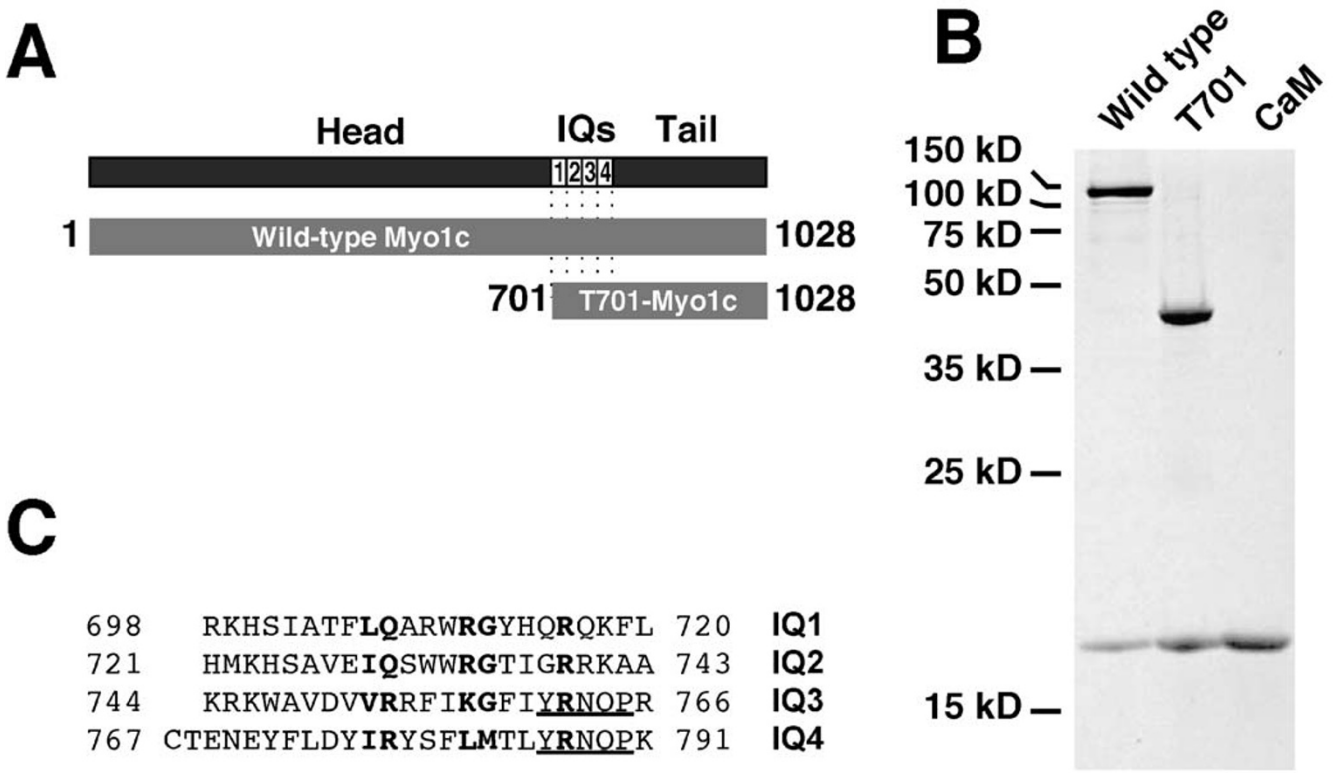

Figure 1
Myo1c constructs and IQ-domain sequences *A*, domain structure of Myo1c, indicating amino acids encompassed by full-length Myo1c and T701-Myo1c constructs. *B*, SDS-PAGE of 15 pmol each of purified full-length Myo1c and T701-Myo1c constructs co-expressed with calmodulin, and calmodulin alone (CaM; 45 pmol) on a 18% acrylamide gel. Molecular mass markers indicated on left. *C*, aligned bullfrog Myo1c IQ domains. The IQ motif positions are in bold and the repeat present in IQ3 and IQ4 is underlined. Numbers indicate amino-acid residue positions.

IQ – calmodulin interaction by quenching of Alexa-calmodulin fluorescence

As noted above, Alexa-calmodulin fluorescence was quenched upon binding to an IQ peptide (Fig. 3A). Because an excess of unlabeled calmodulin was able to reverse 70–95% of the quench (Fig. 3A), we inferred that most Alexa-calmodulin bound to the same site as unlabeled calmodulin. We used this fluorescence-intensity quench empirically to measure the affinity of each IQ peptide for Alexa-calmodulin (Fig. 3B). In some experiments, Ca^{2+} was held at <30 nM by chelation with 100 μM EGTA; in other experiments, we added 25 μM exogenous $CaCl_2$ in the absence of EGTA. These two concentrations mimic the low- and high-Ca^{2+} conditions that Myo1c may encounter in hair cells when the transduction channel is closed or open [26]. In the presence of 100 μM EGTA, K_d values followed the order IQ3 < IQ1 ≈ IQ2 << IQ4. Although the data were fit somewhat better with a modified Hill equation that with a standard bimolecular-binding isotherm (Fig. 3B), the physiological significance of Hill coefficients >1 is uncertain, particularly given the 1:1 peptide:calmodulin stoichiometry (see below). Ca^{2+} had only modest effects on the affinity of the Myo1c IQ peptides for Alexa-calmodulin (Table 1).

Despite only minor effects on binding affinity, Ca^{2+} did influence the calmodulin-peptide complex, as signaled by changes in Alexa-calmodulin fluorescence. Changes in fluorescence intensity during manipulation of a single parameter, like Ca^{2+} concentration, should report conformational changes in Alexa-calmodulin. For example, the fluorescence intensity of free Alexa-calmodulin in solution was ~15% lower in 25 μM $CaCl_2$ than in 100 μM EGTA (left-hand limits in Fig. 4). Because the dye moiety itself is not Ca^{2+} sensitive [27], the Ca^{2+}-dependent fluorescent change reflects changes in the dye's surrounding environment, probably signaling the compact-to-open structural change seen when Ca^{2+} binds to calmodulin [28]. In contrast to the reduction of free Alexa-calmodulin fluorescence by Ca^{2+}, fluorescence of Alexa-calmodulin when saturated by IQ peptides was 1.5- to 2-fold *greater* in 25 μM $CaCl_2$ than in 100 μM EGTA (Fig. 4; Table 1). Thus,

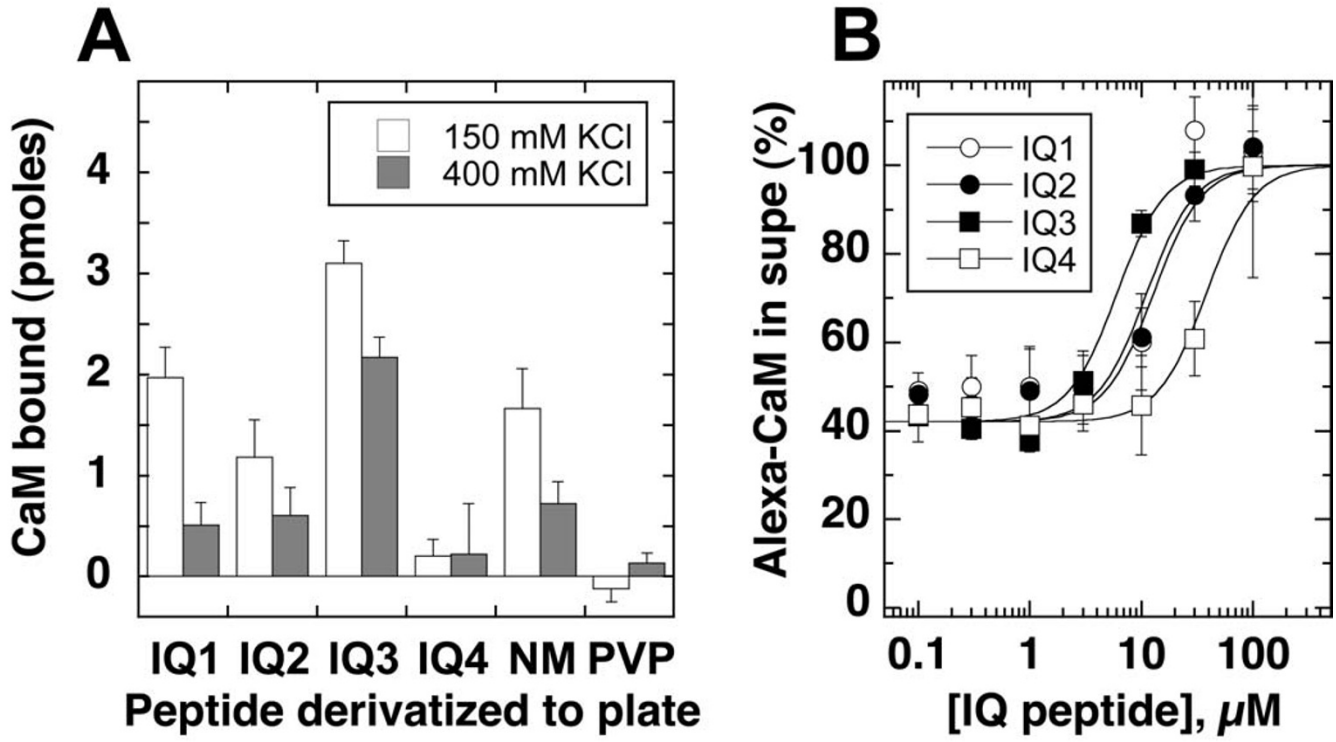

Figure 2
Alexa-calmodulin binding to Myo1c IQ peptides on plates *A*, Alexa-calmodulin (50 nM) was incubated in a 96-well plate covalently bound with Myo1c IQ peptides, a positive-control IQ peptide (NM), or a negative-control peptide (PVP); binding was carried out at room temperature in the presence of low (150 mM) or high (400 mM) KCl and in the presence of 100 μM EGTA. We measured unbound Alexa-calmodulin concentration by fluorescence, then inferred the amount bound. Averaged data from three independent experiments (error bars indicate standard error). *B*, competition with free IQ peptides. Following incubation of 50 nM Alexa-calmodulin and free IQ peptides in the presence of 100 μM EGTA and 150 mM KCl in wells of an IQ3-derivatized plastic plate, unbound Alexa-calmodulin was measured; error bars indicate standard deviation with n = 6 (single experiment). To correct for quenching of Alexa-calmodulin fluorescence by IQ peptides, each sample was standardized against an identical reaction in an underivatized plate. Data were fit with equation (4) with the Hill coefficient set at 2.

when Alexa-calmodulin was bound to IQ peptides, Ca^{2+} induced a conformational change that was substantially different from that seen in the peptide-free state.

IQ – calmodulin interaction under stoichiometric-titration conditions

To determine the affinities of the Myo1c IQ peptides for unlabeled calmodulin, we used Alexa-calmodulin as a reporter (Alexa-calmodulin : unlabeled calmodulin ratio of 1:100) in our binding studies. This approach assumes that Alexa-calmodulin is functionally equivalent to unlabeled calmodulin.

We determined affinities by fitting the IQ-peptide concentration vs. fluorescence quench data with an appropriate model. If the IQ peptides bound only Alexa-calmodulin and not unlabeled calmodulin, the K_d and F_{IQ}/F values of Table 1 would have described the fit to the concentration-quench plots. The line derived from these values did not fit the data (Fig. 5), indicating that, as expected, unlabeled calmodulin binds to the Myo1c IQ peptides.

These experimental conditions resembled a stoichiometric titration, where the total concentration of calmodulin was higher than the K_d values for IQ1, IQ2, and IQ3. Under true stoichiometric-titration conditions (fixed concentration of receptor at 100-fold or more than the K_d, varying the ligand concentration up to and beyond the receptor concentration), almost all of the added IQ peptide would bind tightly to calmodulin and linearly decrease the fluorescence; at the point where the IQ-peptide concentration exceeds the calmodulin concentration multiplied by the peptide:calmodulin stoichiometry (m), a plateau in the fluorescence intensity would be reached. Because the relatively weak affinities observed here make such true stoichiometric titration impractical, we used an intermediate concentration of calmodulin (50 μM, ~10-

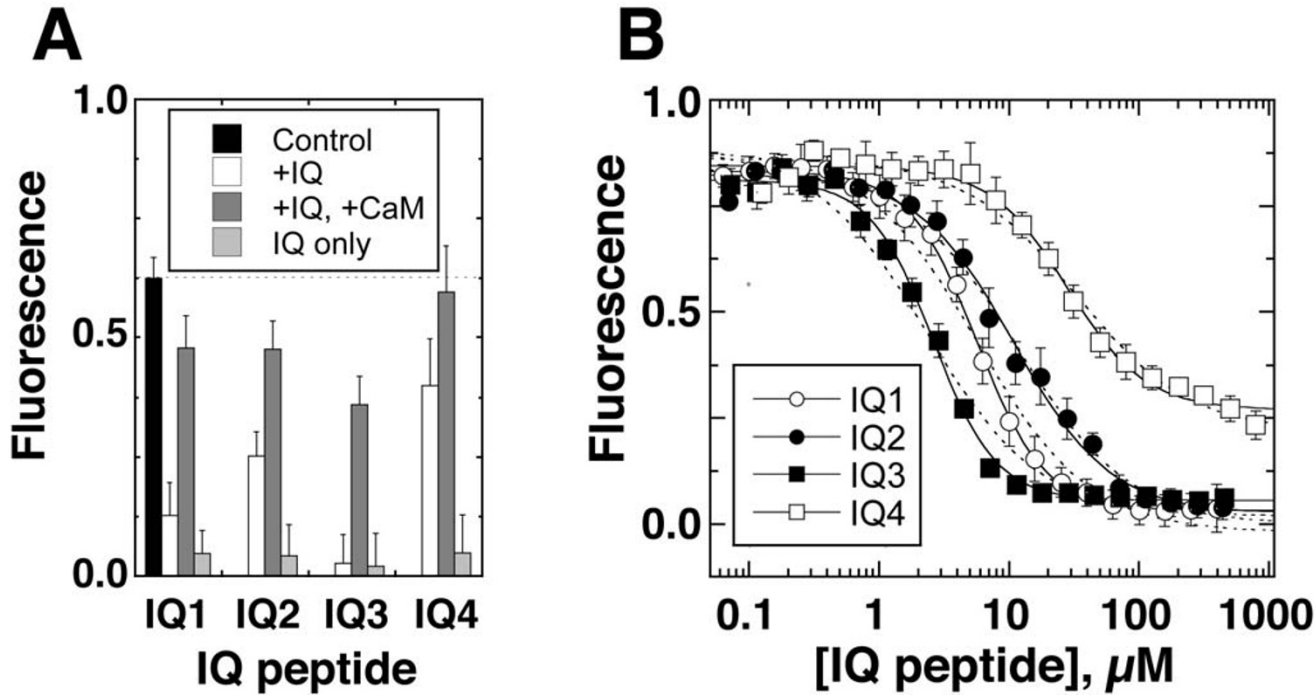

Figure 3

Alexa-calmodulin binding to Myo1c IQ peptides in solution Binding of IQ peptides to Alexa-calmodulin (100 nM) at room temperature with 150 mM KCl and 100 μM EGTA. *A*, IQ peptides quench Alexa-calmodulin fluorescence; unlabeled calmodulin reverses the quench. IQ peptides (25 μM) and unlabeled calmodulin (75 μM) were added as indicated. Control, Alexa-calmodulin alone; +IQ, Alexa-calmodulin plus IQ peptide; +IQ, +CaM, IQ peptide plus unlabeled calmodulin; IQ only, IQ peptides with no Alexa-calmodulin. *B*, Alexa-calmodulin (100 nM) was incubated with increasing concentrations of soluble IQ peptides. Total IQ peptide concentration added is plotted versus Alexa-calmodulin fluorescence, reported in arbitrary fluorescence units; error bars indicate standard deviation with n = 4. Data were fit with equation (3) (dashed lines) and equation (4) (solid lines).

Table 1: Interaction of Myo1c IQ peptides with Alexa-calmodulin

Peptide	K_d, EGTA	F_{IQ}/F, EGTA	K_d, $CaCl_2$	F_{IQ}/F, $CaCl_2$
IQ1	7.3 ± 1.2 μM	0.14 ± 0.02	9.2 ± 1.0 μM	0.39 ± 0.07
IQ2	9.3 ± 1.4 μM	0.21 ± 0.05	6.4 ± 1.4 μM	0.50 ± 0.05
IQ3	2.0 ± 0.4 μM	0.23 ± 0.03	1.3 ± 0.4 μM	0.47 ± 0.03
IQ4	45 ± 5 μM	0.36 ± 0.10	37 ± 19 μM	0.71 ± 0.02

Quenching of Alexa-calmodulin fluorescence was used to estimate binding affinity of IQ peptides to calmodulin using equation (3). F_{IQ}/F is the ratio of Alexa-calmodulin fluorescence in the presence of IQ peptides (extrapolated to saturating peptide) to fluorescence in the absence of peptide. Values reported are means ± standard error (n = 4 independent experiments for each value).

fold larger than K_d) and used equation (7) to describe the equilibrium precisely. This approach allowed us to determine both *m* and K_d in the same experiment.

In the presence of EGTA, the IQ1, IQ2, and IQ3 binding data were much better fit by *m* = 1 than they were to *m* = 2, indicating that the binding stoichiometry of peptide to calmodulin was 1:1 (Fig. 5). The K_d values determined with equation (7) were very similar to those determined for binding to Alexa-calmodulin alone (Tables 1 and 2), confirming that under these conditions, the IQ peptides bind to unlabeled calmodulin and Alexa-calmodulin similarly.

In the presence of Ca^{2+}, IQ3 also bound to calmodulin with a stoichiometry of 1:1 (Fig. 5). The fits to *m* = 1 and 2 were equally good for IQ1 and IQ2 in the presence of Ca^{2+}, signifying the inability for this analysis to determine precise binding stoichiometry of IQ1 and IQ2 under these conditions. In addition, these data indicate that the apparent affinities of IQ1 and IQ2 for unlabeled calmodulin were substantially weakened by Ca^{2+} (Table 2), unlike results with Alexa-calmodulin alone (Table 1). Because the assumption that affinities of Alexa-calmodulin and unlabeled calmodulin for IQ peptides are identical was violat-

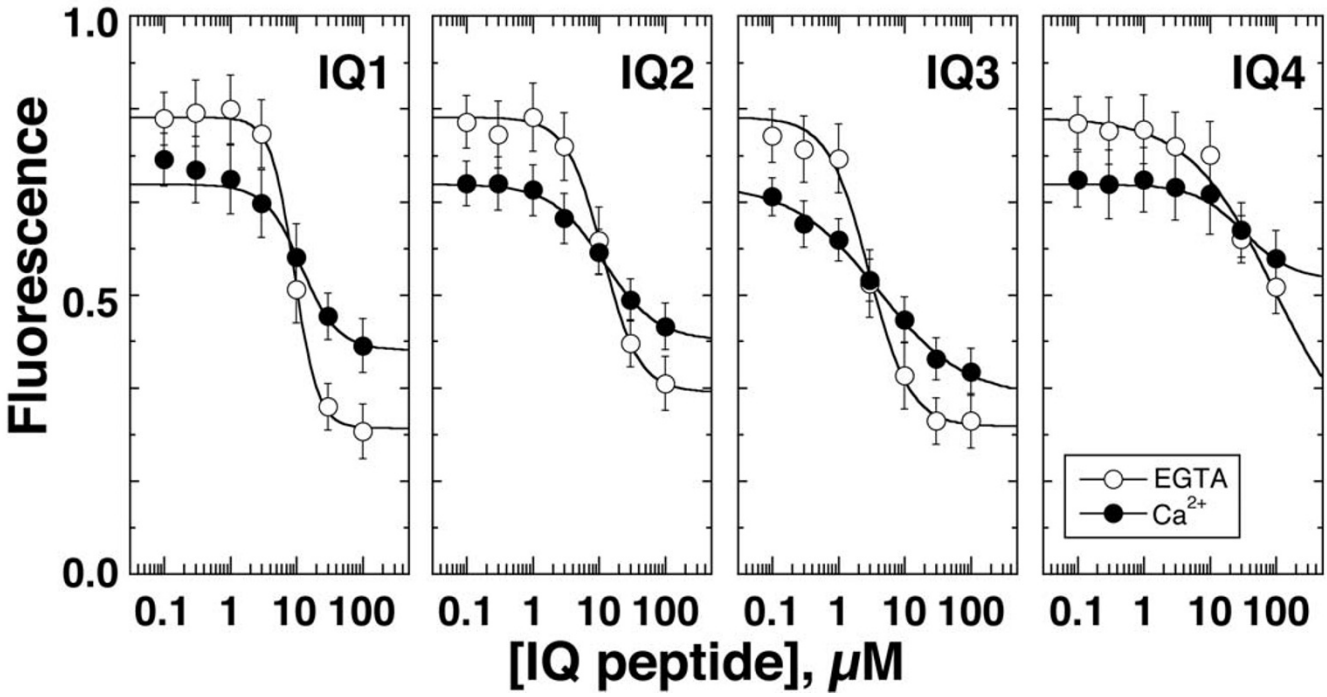

Figure 4
Ca^{2+}-dependence of IQ-Alexa-calmodulin interaction Binding of IQ peptides to Alexa-calmodulin (50 nM) in 100 μM EGTA or 25 μM $CaCl_2$ as described for Fig. 3; error bars indicate standard deviation with n = 6. Data were fit with a modified Hill equation (equation (4)).

ed for IQ1 and IQ2, the actual affinities of these IQ peptides for unlabeled calmodulin may be even weaker than those reported in Table 2. By contrast, Ca^{2+} had only a very modest effect on IQ3 affinity for unlabeled calmodulin.

Binding of IQ4 to unlabeled calmodulin was distinct from that of the other IQ peptides. The data with IQ4 were best fit with a Hill equation (equation 4), with a Hill coefficient of greater than 2 (Fig. 5, thick solid lines), suggesting that binding of two peptides per calmodulin may be required for the fluorescence change. The apparent affinities (~100 μM) were similar to the concentration of calmodulin (50 μM), however, indicating that the apparent affinities did not accurately reflect K_d values. These results with a mixture of unlabeled and Alexa-calmodulin were different from those with Alexa-calmodulin alone, where IQ4 Hill coefficients were close to 1 (data not shown). Nevertheless, these data show that unlabeled calmodulin can bind to IQ4, albeit with weak affinity and uncertain stoichiometry.

Hydrodynamic analysis of full-length Myo1c

To determine the stoichiometry and Ca^{2+}-dependent regulation of calmodulin binding to Myo1c with all four IQ motifs, we co-expressed calmodulin and full-length bullfrog Myo1c in insect cells using baculoviruses and subjected the purified Myo1c-calmodulin complexes (Fig. 1B) to hydrodynamic analysis (Table 3). We carried out velocity sedimentation of Myo1c-calmodulin complexes on 5–20% sucrose gradients to determine sedimentation coefficients. We measured the Stokes radius of Myo1c-calmodulin complexes using gel filtration on Superdex 200 under temperature and buffer conditions identical to those of the velocity-sedimentation experiments (Table 3). Although most experiments used 400 mM KCl (which prevented adsorption to the gel-filtration matrix), we obtained identical sedimentation coefficients in the presence of 150 or 250 mM KCl (not shown). Velocity-sedimentation and gel-filtration experiments were carried out at 4°C, the temperature used for Myo1c purification, as well as at 25°C, a physiologically relevant temperature for a bullfrog.

To calculate the molecular mass of Myo1c-calmodulin complexes, we applied the modified Svedberg equation, which relates mass to the diffusion constant (calculated here from Stokes radius) and the sedimentation coefficient [29]. The partial specific volume of each protein complex was determined using the amino-acid composition of the constituent proteins (Table 3; ref. [30]). Although the uncertainty in calmodulin stoichiometry leads

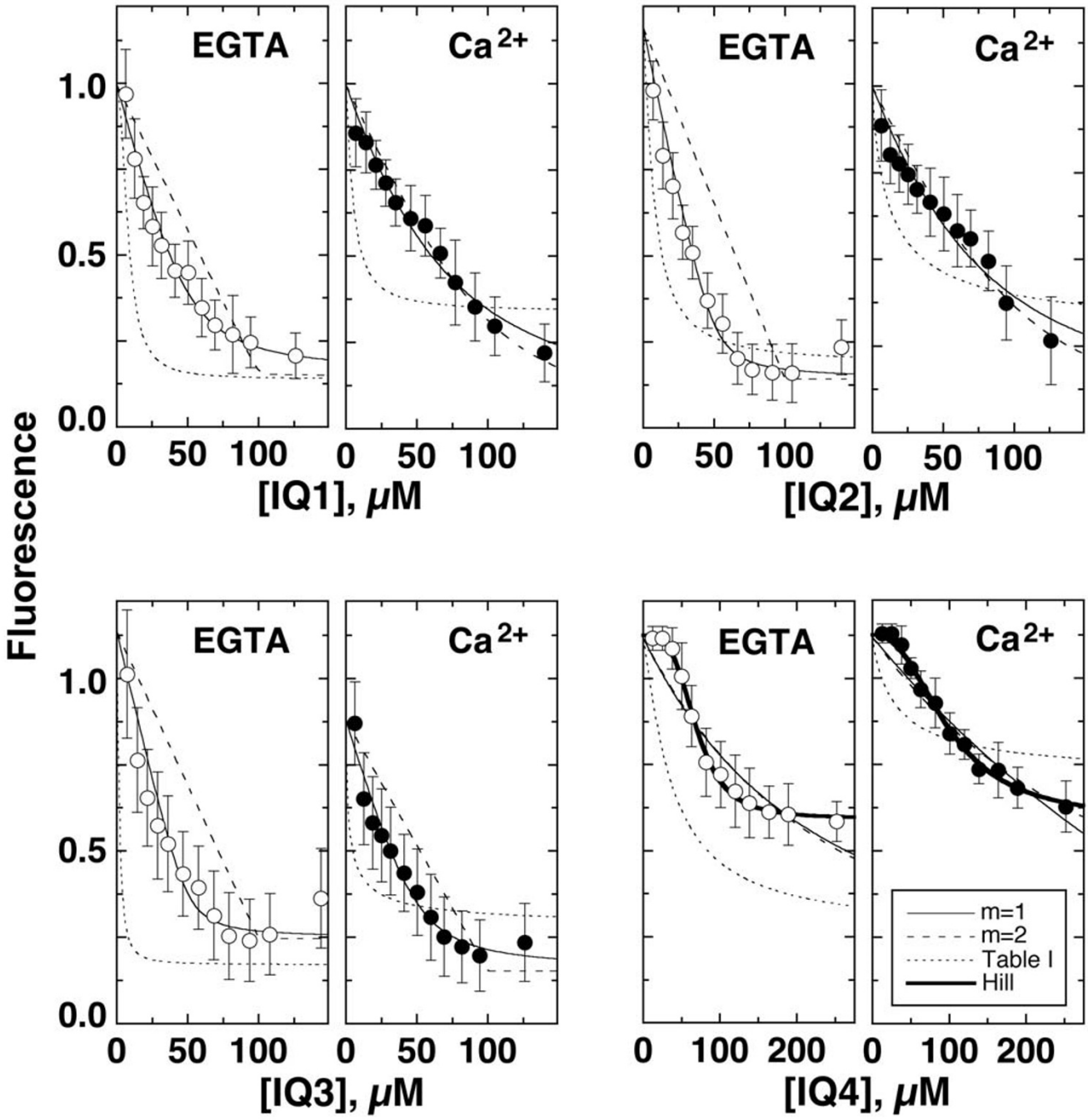

Figure 5
Binding of unlabeled calmodulin to Myo1c IQ peptides Fluorescence intensity during titration of a mixture of 50 μM unlabeled calmodulin and 500 nM Alexa calmodulin (used as a reporter) with IQ peptides (total concentration). Thin solid lines: fit with equation (7) assuming m = 1. Dashed lines: fit with equation (7) assuming m = 2 and final fluorescence from m = 1 fit. Dotted lines: results predicted from Table 1 if unlabeled calmodulin does not affect the Alexa-calmodulin – IQ peptide equilibrium. Thick solid lines (IQ4 only): fit with equation (4). Error bars indicate standard deviation with n = 4. Note difference in the abscissa scale for IQ4.

Table 2: Interaction of Myo1c IQ peptides with unlabeled calmodulin

Peptide	Apparent K_d, EGTA	Apparent K_d, $CaCl_2$
IQ1	4.0 ± 0.8 μM	56 ± 13 μM
IQ2	4.2 ± 2.0 μM	70 ± 15 μM
IQ3	1.7 ± 0.7 μM	3.2 ± 1.1 μM

Quenching of Alexa-calmodulin fluorescence was used to estimate binding affinity of IQ peptides to calmodulin using equation (7). Values reported are means ± standard error (n = 3 to 4 independent experiments for each value). IQ4 affinities were not accurately measured under conditions of this assay, but were >100 μM.

to ambiguity in this calculation, the calculated partial specific volumes were so close (*e.g.*, 0.734 for one and 0.731 for three calmodulins per Myo1c complex) that the precise value did not significantly affect the final molecular-mass value.

Full-length Myo1c bound ~3 calmodulins per Myo1c at 4°C in the presence of EGTA or $CaCl_2$ (Table 3). One of the bound calmodulins was only weakly associated, as elevation of the temperature to 25°C induced the release of 1 mole of calmodulin in the presence of EGTA. When Ca^{2+} was elevated to 25 μM at 25°C, however, we could not detect substantial full-length Myo1c in solution after sucrose-gradient centrifugation or gel filtration, suggesting that the protein had aggregated.

Hydrodynamic analysis of T701-Myo1c

Because the size of full-length Myo1c (125 kD, including purification and detection tags) is much larger than calmodulin (16.7 kD), we improved our ability to determine stoichiometry from molecular mass by examining a smaller (45 kD) neck-tail recombinant fragment of Myo1c. This construct, T701-Myo1c, contained amino acids 701–1028 of bullfrog Myo1c, including all four IQ domains, the entire C-terminal tail, and N-terminal purification and epitope tags (Fig. 1A,1B).

T701-Myo1c bound 2.5 moles of calmodulin per mole of heavy chain at 4°C in the presence of 100 μM EGTA (Fig. 6; Table 4). As with full-length Myo1c, elevation of the analysis temperature to 25°C induced the release of ~0.7 mole of calmodulin. In contrast to the results seen with full-length Myo1c, elevation of the $CaCl_2$ concentration to 25 μM at 4°C also induced the release of ~0.7 mole of calmodulin. The amount of T701-calmodulin complex recovered on sucrose gradients or by gel filtration decreased substantially when the $CaCl_2$ concentration was elevated to 25 μM at 25°C, signaling the formation of aggregates, as seen with the full-length complex. Furthermore, the calculated calmodulin stoichiometry of the observed T701-calmodulin complex under these conditions was only ~0.3 mole of calmodulin per mole of Myo1c, reinforcing the suggestion that Ca^{2+} induced the dissociation of most calmodulins at 25°C and that this loss of light chains resulted in aggregation.

Table 3: Hydrodynamic analysis of full-length Myo1c

Property	Temperature	Full-length Myo1c 100 μM EGTA	Full-length Myo1c 25 μM $CaCl_2$
Sedimentation coefficient	4°C	6.70 ± 0.07 S (n = 5)	6.90 ± 0.08 S (n = 4)
	25°C	6.28 ± 0.21 S (n = 8)	*
Stokes radius	4°C	6.06 ± 0.08 nm (n = 7)	6.07 ± 0.05 nm (n = 4)
	25°C	5.78 ± 0.11 nm (n = 5)	*
Molecular mass	4°C	168 ± 4 kD	4°C: 173 ± 3 kD
	25°C	150 ± 7 kD	ND
Frictional ratio	4°C	1.7 ± 0.1	1.7 ± 0.1
	25°C	1.7 ± 0.1	ND
Calmodulins per molecule	4°C	2.5 ± 0.2	2.9 ± 0.2
	25°C	1.5 ± 0.4	ND

* Very low levels of protein detected.

Full-length Myo1c was co-expressed with calmodulin, purified, and subjected to sucrose-gradient centrifugation or gel-filtration analysis. Myo1c was detected by ELISA (sucrose gradients) or by absorption at 280 nm (gel filtration). Molecular mass was determined using the Stokes-Einstein equation; the number of calmodulins was estimated by subtracting the mass of the Myo1c heavy chain from the estimated molecular mass, then dividing the remainder by the mass of calmodulin (16.7 kD). Values reported are mean ± standard deviation. ND, not determined.

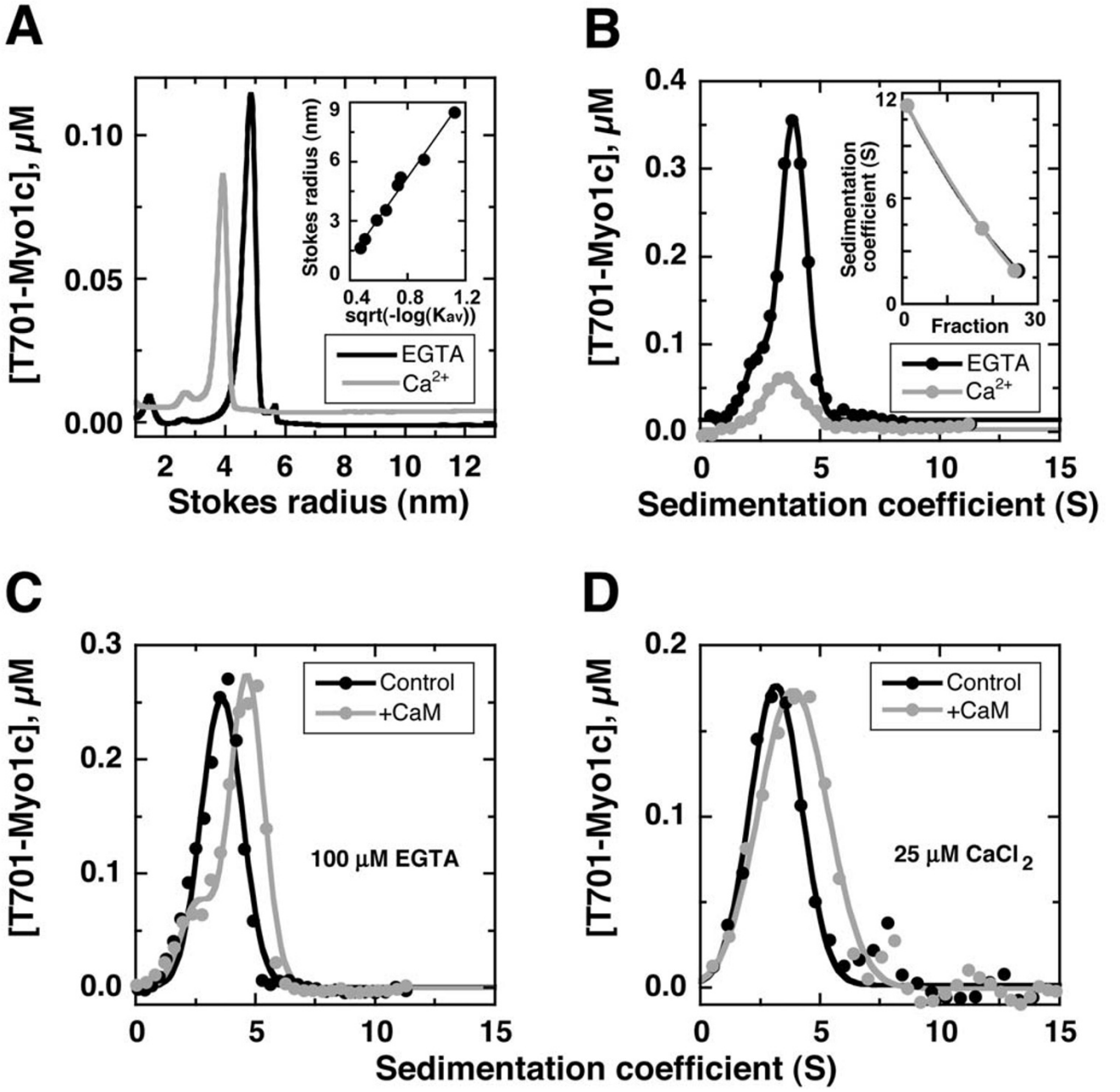

Figure 6

Hydrodynamic analysis of T701-Myo1c *A*, measurement of Stokes radius using gel filtration. Globular standards were used to calibrate the column, and retention times were converted to Stokes radius (inset). T701-Myo1c was separated at 25°C in the presence of 100 μM EGTA (Stokes radius of 4.8 nm) or 25 μM $CaCl_2$ (3.9 nm). *B-D*, measurement of sedimentation coefficients using sucrose-gradient centrifugation. Size standards were used to calibrate the gradient, and fraction numbers were converted to sedimentation coefficient (inset, panel B). T701-Myo1c concentration was determined by ELISA. *B*, T701-Myo1c sedimentation at 4°C in the presence of 100 μM EGTA (3.9 S) or 25 μM $CaCl_2$ (3.5 S). *C*, T701-Myo1c sedimentation in the presence of EGTA at 25°C, with (4.6 S) or without (3.8 S) the continuous presence of 5 μM calmodulin (+CaM). *D*, T701-Myo1c sedimentation in the presence of 25 μM $CaCl_2$ at 25°C, with (3.9 S) or without (3.1 S) the continuous presence of 5 μM calmodulin.

Table 4: Hydrodynamic analysis of T701-Myo1c.

Property	Temperature	T701-Myo1c 100 μM EGTA	T701-Myo1c 25 μM $CaCl_2$
Sedimentation coefficient	4°C	4.64 ± 0.11 S (n = 4)	4.27 ± 0.21 S (n = 3)
	25°C	3.83 ± 0.06 S (n = 11)	3.13 ± 0.30 S (n = 7)
Stokes radius	4°C	4.52 ± 0.06 nm (n = 4)	4.19 ± 0.11 nm (n = 6)
	25°C	4.74 ± 0.13 nm (n = 6)	3.78 ± 0.07 nm (n = 6)
Molecular mass	4°C	87 ± 5 kD	74 ± 6 kD
	25°C	75 ± 3 kD	49 ± 5 kD
Frictional ratio	4°C	1.5 ± 0.1	1.5 ± 0.1
	25°C	1.7 ± 0.1	1.6 ± 0.2
Calmodulins per molecule	4°C	2.5 ± 0.1	1.8 ± 0.2
	25°C	1.8 ± 0.2	0.3 ± 0.3

Analysis was carried out as described for Table 3 using purified T701-Myo1c.

Table 5: Hydrodynamic analysis of T701-Myo1c in the presence of 5 μM calmodulin

Property	Temperature	T701-Myo1c 100 μM EGTA	T701-Myo1c 25 μM $CaCl_2$
Sedimentation coefficient	25°C	4.68 ± 0.11 S (n = 2)	3.95 ± 0.33 S (n = 4)
Molecular mass	25°C	92 ± 4 kD	62 ± 12 kD
Calmodulins per molecule	25°C	2.8 ± 0.2	1.0 ± 0.7

Purified T701-Myo1c co-expressed with calmodulin, was subjected to sucrose-gradient centrifugation in the presence of 5 μM calmodulin in either 100 μM EGTA or 25 μM $CaCl_2$. T701-Myo1c was detected by ELISA. We estimated molecular mass and hence stoichiometry by assuming that Stokes radii of the complexes were unchanged by the presence of calmodulin, an assumption that might have led to an underestimate of the mass. Values reported are mean ± range or standard deviation.

We could not prevent the release of calmodulin at 25°C by saturating T701-Myo1c with excess calmodulin immediately prior to centrifugation (preloading). In EGTA, the sedimentation coefficient of calmodulin-preloaded T701-Myo1c measured at 25°C (3.85 ± 0.07 S; n = 2) was nearly identical to that measured without preloading (3.83 S; Table 4). Likewise, the sedimentation coefficient of calmodulin-preloaded T701-Myo1c measured at 25°C and in 25 μM $CaCl_2$ (2.80 ± 0.42 S; n = 2) was similar to that measured without preloading (3.13 S; Table 4).

By contrast, we could prevent the temperature-dependent loss of calmodulin by carrying out sedimentation in the continuous presence of 5 μM calmodulin (Fig. 6C,6D; Table 5). Although gel-filtration analysis was impractical with this high calmodulin concentration, we assumed that the Stokes radius of T701-Myo1c in the presence of calmodulin was identical to the value obtained in the absence. Sedimentation at 25°C in EGTA gradients supplemented with 5 μM calmodulin resulted in the retention of ~3 calmodulins per T701-Myo1c. In 25 μM $CaCl_2$, supplementation with 5 μM calmodulin resulted in ~1 calmodulin bound per T701-Myo1c. In addition, protein loss due to aggregation was minimal under these conditions.

Myo1c-calmodulin stoichiometry by gel scanning

To measure Myo1c-calmodulin stoichiometry by an independent method, we separated calmodulin standards and T701-Myo1c by SDS-PAGE (Fig. 7A). Using densitometry, we quantified the staining intensity of the calmodulin standards to generate a standard curve (Fig. 7B) and determined the amount of calmodulin present in each T701-Myo1c sample. Applying the analysis described in Experimental Procedures and equation (13), we found an average of 2.6 ± 0.2 calmodulins per T701-Myo1c (mean ± standard error) in six experiments, three separate prepara-

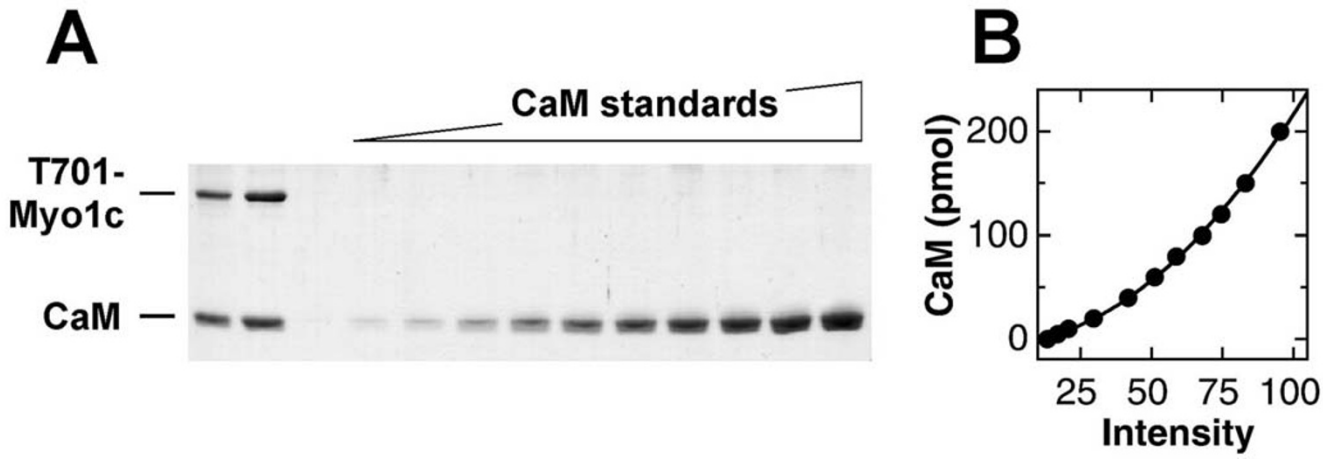

Figure 7
Myo1c-calmodulin stoichiometry by gel scanning *A*, Coomassie-stained SDS-PAGE gel with two independent T701-Myo1c preparations (left lanes) and dilutions of purified bovine-brain calmodulin (CaM). *B*, calmodulin standard curve derived by gel scanning.

tions analyzed in duplicate. This value was very close to the value of 2.5 ± 0.1 bound calmodulins determined independently by hydrodynamic analysis (Table 4).

Discussion

Calmodulin interaction with individual Myo1c IQ domains

To examine how calmodulin binds to the Myo1c IQ sites, we developed two binding assays using a commercially available fluorescent calmodulin and individual IQ peptides. In one assay, we covalently attached peptides to plastic plates, then measured the amount of fluorescent calmodulin that remained unbound after incubation with the peptide-derivatized plate. This assay was simple and fast, and allowed us to measure binding under a wide variety of conditions. In our second assay, we exploited the empirical observation that the Alexa-calmodulin fluorescence intensity is quenched by binding of IQ peptides. As in other assays with fluorescently labeled calmodulins (e.g., ref. [31]), binding of the peptides to Alexa-calmodulin did not perfectly mimic binding to unlabeled calmodulin. For example, Alexa-calmodulin bound IQ peptides more strongly in the presence of Ca^{2+} than did unlabeled calmodulin. Moreover, excess unlabeled calmodulin could not fully reverse the quenching of Alexa-calmodulin fluorescence induced by IQ peptides, suggesting that IQ peptides could bind to Alexa-calmodulin at two sites, including one where unlabeled calmodulin could not bind. Indeed, binding of IQ peptides to both sites on a single fluorescent calmodulin could account for Hill coefficients of >1 seen in some experiments (e.g., Figs. 3B and 4). Nevertheless, these discrepancies should not prevent use of Alexa-calmodulin for measuring interaction with calmodulin's targets, particularly if the interaction with unlabeled calmodulin is compared to the interaction with Alexa-calmodulin.

Calmodulin bound to peptides corresponding to each of the four Myo1c IQ domains, although with differing affinity and Ca^{2+} sensitivity. Affinities for calmodulin binding to IQ1 and IQ2 were relatively modest (K_d values of ~5 μM). As with other IQ domains [14], Ca^{2+} weakened the affinity of calmodulin for IQ1 and IQ2 by more than 10-fold.

By contrast, calmodulin binding to IQ3 was slightly stronger and was affected much less by Ca^{2+}. Because calmodulin binds strongly to classic IQ domains only in the absence of Ca^{2+} [14,32], its strong binding to IQ3 in the presence of Ca^{2+} suggests the participation of an additional Ca^{2+}-requiring binding motif. Two common calmodulin-binding motifs, called 1-8-14 and 1-5-10 for the pattern of hydrophobic amino-acid residues, require Ca^{2+} for calmodulin binding [14]. IQ3 has two nearly perfect 1-5-10 domains that are at +2 net charge instead of the minimum +3 in the consensus [14]. In addition, IQ3 has a 1-8-14 motif with a proline residue at position 14 instead of phenylalanine, isoleucine, leucine, valine, or tryptophan. Because most proteins that bind calmodulin through the 1-8-14 and 1-5-10 motifs do so strongly, the relatively modest affinity of IQ3 for calmodulin in the presence of Ca^{2+} suggests that calmodulin binds through one of these imperfect motifs located within this IQ domain. To interact with an alternate set of residues, Ca^{2+}-calmodulin must adopt a new conformation. A similar Ca^{2+}-dependent rearrangement was predicted for the complex of calmodulin and the first IQ domain of myosin-1a (brush-border myosin I) [32].

In support of this view, we observed evidence for Ca^{2+}-dependent conformational changes in calmodulin while bound to IQ peptides. When Alexa-calmodulin was bound to Myo1c IQ peptides, its fluorescence was higher in the presence of Ca^{2+} than in its absence, suggesting that that Ca^{2+}-bound Alexa-calmodulin binds to the IQ peptides in a different conformation than does Ca^{2+}-free Alexa-calmodulin. For example, in the absence of Ca^{2+}, Alexa-calmodulin may bind to IQ peptides in a more compact conformation, quenching fluorescence by burying dye moieties in a less polar environment. Although the Ca^{2+}-induced conformational change could be a property of Alexa-calmodulin rather than calmodulin itself, the Ca^{2+}-dependent changes in affinity of calmodulin for IQ1 and IQ2 (Table 2) and calmodulin's likely shift to a new binding site on IQ3 suggests that the conformational change is probably also a property of authentic calmodulin.

Calmodulin also bound to a newly identified domain, IQ4. Because the affinity of calmodulin for IQ4 is very weak, calmodulin should only occupy IQ4 in subcellular locations with a low Ca^{2+} concentration and a high level of free calmodulin. For example, a small population of Myo1c molecules with calmodulin bound to IQ4 should be present in the stereocilia of inner-ear hair cells, which contain ~35 μM free calmodulin [33]. Although most tissues contain less free calmodulin [34], concentrations in other individual organelles can reach the millimolar range [35]. On the other hand, the weak affinity of this IQ domain for calmodulin suggests that IQ4 may play another role, such as interacting with another protein.

Calmodulin interaction with Myo1c

The binding affinities of calmodulin for the individual IQ peptides do not reflect exactly the affinities of calmodulin for the IQ domains within Myo1c. For example, despite micromolar K_d values for calmodulin-IQ peptide interactions, calmodulin remains bound to Myo1c during long gel-filtration or centrifugation experiments, even at nanomolar Myo1c concentrations (Fig. 6). This result suggests that calmodulin binds to some of Myo1c's four tandem IQ domains substantially more strongly than to the individual peptides. For example, other regions of Myo1c could constrain the IQ domains in conformations that are substantially more (or less) favorable for calmodulin binding than the population of conformations adopted by a soluble IQ peptide. Moreover, calmodulin binding to Myo1c could be influenced by interactions with adjacent calmodulin molecules or to the Myo1c head or tail domains.

To examine calmodulin binding to IQ domains in Myo1c, we determined the molecular mass (and hence calmodulin:Myo1c stoichiometry) and shape of Myo1c under the appropriate conditions of temperature and Ca^{2+}. Although analytical ultracentrifugation is more commonly used to measure molecular size of protein-protein complexes [36], we instead used classic hydrodynamic methods of velocity sedimentation on sucrose gradients to obtain sedimentation coefficients and gel filtration to obtain Stokes' radius. One advantage of this approach was that by detecting Myo1c using a sensitive ELISA method, we were able to use very low concentrations of Myo1c. Furthermore, we were able to carry out sedimentation in the presence of a high concentration of calmodulin, a manipulation that prevents Myo1c detection in a standard analytical ultracentrifugation experiment. A disadvantage of this approach was the need for high concentrations of sucrose, which in rare conditions can substantially affect the hydrodynamic properties of a protein [37]; nevertheless, changes in Myo1c size were observed both in velocity sedimentation (in the presence of sucrose) and in gel filtration (in its absence). Another disadvantage of our classic approach to molecular-mass determination was that the gel filtration and velocity sedimentations were done on different time scales (~1 hour vs. 15–18 hours). If calmodulin slowly dissociated during the analysis (which in both assays diluted Myo1c well below 1 μM), the degree of dissociation would be larger in the velocity sedimentation experiments than in the gel filtration experiments. Nevertheless, our approach was validated by the demonstration that the number of calmodulins per T701-Myo1c was identical in hydrodynamic and gel-scanning experiments, at least in EGTA at 4°C.

Because T701-Myo1c mimicked properties of the full-length protein (except under low-temperature, high-Ca^{2+} conditions), we exploited the neck-tail construct for a more detailed analysis of calmodulin binding. As expected from the large Ca^{2+}-dependent weakening of calmodulin affinity for IQ1 and IQ2 (Fig. 5; Table 2), Ca^{2+} decreased the number of calmodulins bound to T701-Myo1c at high ionic strength. When Ca^{2+} was low at 25°C, each T701-Myo1c had about two bound calmodulins, with a third bound if the calmodulin concentration reached 5 μM. At this calmodulin concentration, IQ domains 1, 2, and 3 are likely occupied by calmodulin. When Ca^{2+} is high at 25°C, all but one calmodulin dissociated from T701-Myo1c in the presence of 5 μM free calmodulin. The strong affinity of IQ3 for Ca^{2+}-calmodulin suggests that the remaining calmodulin was bound to this IQ domain.

How many calmodulins are bound to Myo1c in the cell at increased Ca^{2+} concentrations? The elevated ionic strength used for the hydrodynamic analysis probably weakened the affinity of the calmodulin for IQ3 (Fig. 2A), requiring 5 μM free calmodulin to maintain occupancy of that site. We therefore infer that at a physiologically signif-

icant temperature and at a cellular ionic strength, Ca^{2+} triggers release of calmodulins from IQ1 and IQ2 from T701-Myo1c, leaving only IQ3 occupied. Although these results contrast with those reported for mammalian Myo1c, where only one of three calmodulins is released by Ca^{2+} [19,38], our T701 construct lacks Myo1c's motor domain. It is entirely plausible that even in the presence of Ca^{2+}, calmodulin remains bound to IQ1, albeit in a different conformation and dependent on interactions with the myosin head. Our results therefore suggest that Ca^{2+} either induces the release of calmodulin from IQ1 or causes it to change its interaction with Myo1c substantially.

Of the three calmodulins bound to Myo1c, one of these binds relatively weakly at 25°C, even in EGTA. To which IQ domain does this weakly bound light chain bind? Although calmodulin binds to IQs 1–3 with approximately the same strength in the presence of EGTA, we suggest that the readily released calmodulin is likely to be that bound to IQ2. To bind three calmodulins, IQs 1–3, each of which are only 23 amino acids long, must be arranged without kinks [32]; this arrangement may produce unfavorable strain on each of the calmodulin molecules. Release of calmodulin from IQ2 would relieve all of that strain; release from IQs 1 or 3 would not. Strain relief also may accelerate calmodulin release in the presence of Ca^{2+}; because Ca^{2+} apparently rearranges the three-dimensional interaction of calmodulin with IQ3, binding of an adjacent calmodulin – on IQ2 – might be destabilized even more [32].

Despite the loss of calmodulin from T701-Myo1c induced by elevation of the temperature from 4°C to 25°C, the frictional ratio (a measure of the protein's asymmetry) increased (Table 4). The neck-tail region of Myo1c thus appears to adopt a compact structure at 4°C, becoming more extended at 25°C. Less calmodulin may be released at lower temperatures because the Myo1c tail may bind to and stabilize calmodulin's interaction with the Myo1c neck.

Implications for Myo1c activity

The Ca^{2+}-dependent change in interaction of calmodulin with IQ1, the IQ domain closest to the motor domain, has important implications for Myo1c mechanochemical function. Although Ca^{2+} increases Myo1c ATPase activity, the ion completely halts *in vitro* motility [19]. Ca^{2+}-dependent changes in conformation may prevent amplification of a small converter-domain movement into a large motor step. In the presence of an external force, as is seen by Myo1c during an excitatory mechanical stimulus in a hair cell [39], Ca^{2+} (which enters the cell through open transduction channels), should permit Myo1c to go through its ATPase cycle, binding and unbinding from actin, but the altered interaction of calmodulin and IQ1 may prevent force production by the motor. We predict that Ca^{2+} will decrease the stiffness of a Myo1c-actin interaction, preventing coupling of the energy released by ATP hydrolysis to the swing of the neck [40]. This behavior will assist Myo1c in its role of adaptation in hair cells, where the motor reduces force applied to the hair cell's transduction channel.

A limitation of our experiments is the restriction of Myo1c binding to a single type of light chain, calmodulin. Other light chains can interact with IQ domains, including essential light chain isoforms [41] and calmodulin-like protein [42]. Although purified bovine adrenal Myo1c does not appear to have alternative associated light chains [12], we can not rule out the possibility that other light chains bind in a cellular context. Nevertheless, purified recombinant full-length Myo1c associated with calmodulin light chains exhibited actin-activated ATPase activity and motility *in vitro* [43], indicating that calmodulin can function as a Myo1c light chain.

That Myo1c does not bind calmodulin tightly is, at first glance, surprising. Weak calmodulin binding may, however, permit access of IQ domains to intracellular Myo1c receptors. Accordingly, we have found that a Myo1c fragment containing only IQs 1–3, partially complexed with calmodulin, binds avidly to hair-cell receptors; excess calmodulin blocks this interaction, probably by binding to an unoccupied IQ site on the Myo1c fragment [13]. IQ2 is highly conserved between species, leading us to propose that hair-cell receptors interact through this region [13]. Because Myo1c-interacting proteins in hair cells and elsewhere may interact through IQ domains, regulation of calmodulin binding to Myo1c – for example, by Ca^{2+} – likely affects coupling of the motor protein to its cargo.

Conclusions

Under low Ca^{2+} conditions and normal ionic strength, calmodulin binds moderately tightly to three Myo1c IQ domains, IQ1, IQ2, and IQ3. IQ4 will only be occupied when the calmodulin concentration is very high. When linearly arranged in the Myo1c molecule, at least one calmodulin (most likely that bound to IQ2) is bound less tightly, probably due to steric constraints. Upon binding Ca^{2+}, calmodulin bound to IQ2 dissociates; that bound to IQ1 either dissociates or changes its conformation sufficiently that chemomechanical coupling cannot ensue.

Methods

Peptide – calmodulin interaction on plates

Bullfrog Myo1c IQ peptides were synthesized (Genemed Synthesis, South San Francisco, CA) with N-terminal cysteine residues: IQ1 (residues 698–720), CRKHSIATFLQARWRGYHQRQKFL; IQ2 (721–743), CHMKHSAVEIQSWWRGTIGRRKAA; IQ3 (744–766),

CKRKWAVDVVRRFIKGFIYRNQPR; and IQ4 (767–791; native cysteine at residue 767), CTENEYFLDYIRYSFLMTLYRNQPK. Peptide concentrations were measured by determining optical density at 280 nm, using calculated molar extinction coefficients of 7090 (IQ1), 11500 (IQ2), 7090 (IQ3), and 5240 M^{-1} cm^{-1} (IQ4). We also synthesized a negative-control peptide ("PVP") corresponding to amino acids 792–816 of frog Myo1c (SVLDKSWPVPPPSLREASELLREMC; native C816) and a positive control IQ-peptide ("NM") corresponding to amino acids 29–52 of bovine neuromodulin with an added C-terminal cysteine (KAHKAATKIQASFRGHITRKKLKC) [24].

For measuring interaction of calmodulin with peptides conjugated to plastic plates, we incubated 10 μM peptide in phosphate-buffered saline (PBS; 137 mM NaCl, 2.7 mM KCl, 4.3 mM Na_2HPO_4, 1.4 mM KH_2PO_4, pH 7.4) overnight at room temperature in a maleimide-derivatized 96-well plate (Pierce, Rockford, IL). Peptide was present in large excess over free binding sites (25–50 pmol) on the plates. To remove unconjugated peptides, plates were washed with PBS; unreacted sites were saturated by incubating with 10 μg/ml cysteine for 1 hour. We then incubated the peptide-conjugated plates with 50 nM Alexa Fluor 488 calmodulin (Alexa-calmodulin; Molecular Probes, Eugene, OR) in 100 μl of a solution that contained 150 or 400 mM KCl, 1 mM $MgCl_2$, 100 μM ethylene glycol-bis(β-aminoethylether)-N,N,N',N'-tetraacetic acid (EGTA) or 25 μM $CaCl_2$, and 15 mM 2-[4-(2-hydroxyethyl)-1-piperazinyl] ethanesulfonic acid (HEPES) at pH 7.5. According to the manufacturer, Alexa-calmodulin had two dye moieties per calmodulin molecule; the modified residues were likely Lys-75 and Lys-94, the most reactive of calmodulin's lysine residues [44]. After incubation for 2 hours at room temperature, we transferred 50 μl of the solution to another 96-well plate and measured fluorescence (excitation 485 nm; emission, 520 nm) using a BMG Labtechnologies Fluorostar 403 microplate fluorometer (Durham, NC). Under the assay conditions, the inner-filter effect (absorption of excitation or emission photons by the sample) was negligible. From this measurement, we calculated the amount of calmodulin bound to the conjugated peptides. In some experiments, we also included 0.1–100 μM unconjugated IQ peptide; in that case, we carried out duplicate control reactions in underivatized 96-well plates to correct for fluorescence quenching exerted by IQ peptides.

Peptide – calmodulin interaction by fluorescence quench

We used empirically observed changes in the fluorescence intensity of Alexa-calmodulin, large in magnitude, to measure binding of IQ peptides to calmodulin. Peptides and 50–500 nM Alexa-calmodulin were mixed in 96- or 384-well microtiter plates with 150 mM KCl, 1 mM $MgCl_2$, 100 μM EGTA or 25 μM $CaCl_2$, 0.5 mg/ml bovine serum albumin, and 15 mM HEPES at pH 7.5; in some experiments we added 50–75 μM bovine-brain calmodulin. Total volume varied from 10 μl (384-well plates) to 100 μl (96-well plates). After 1–2 hours at room temperature, fluorescence was read directly.

When IQ peptides bound to Alexa-calmodulin, the fluorescence intensity was reduced as the quantum yield decreased (fluorescence quenching). We assumed that two fluorescent species were present, Alexa-calmodulin and IQ peptide-bound Alexa-calmodulin, and that the fluorescence intensity (I) was a linear combination of the fluorescence of the two species:

$$I = f_{\mathrm{CaM}} I_{\mathrm{CaM}} + f_{\mathrm{CaM\text{-}IQ}} I_{\mathrm{CaM\text{-}IQ}} \quad (1)$$

where f_{CaM} and $f_{\mathrm{CaM\text{-}IQ}}$ are the mole fractions of the two components and I_{CaM} and $I_{\mathrm{CaM\text{-}IQ}}$ are their fluorescence intensities. Because the quantum yield of Alexa-calmodulin is reduced when IQ peptides bind, $I_{\mathrm{CaM\text{-}IQ}} < I_{\mathrm{CaM}}$. The fraction of peptide bound is:

$$f_{\mathrm{CaM\text{-}IQ}} = 1 - \frac{I - I_{\mathrm{CaM\text{-}IQ}}}{I_{\mathrm{CaM}} - I_{\mathrm{CaM\text{-}IQ}}} \quad (2)$$

To calculate K_d, we fit the data with a bimolecular-binding isotherm:

$$I = \left(I_{\mathrm{CaM}} - I_{\mathrm{CaM-IQ}}\right) \cdot \left(1 - \frac{[\mathrm{IQ}]}{[\mathrm{IQ}] + K_d}\right) + I_{\mathrm{CaM-IQ}} \quad (3)$$

where [IQ] was the free IQ-peptide concentration added. Because we used concentrations of Alexa-calmodulin in our experiments that were much less than the K_d, we approximated [IQ] using the total IQ peptide concentration.

In other cases, however, the binding data were fit better with a modified Hill equation:

$$I = \left(I_{\mathrm{CaM}} - I_{\mathrm{CaM-IQ}}\right) \cdot \left(1 - \frac{[\mathrm{IQ}]^h}{[\mathrm{IQ}]^h + K_d{}^h}\right) + I_{\mathrm{CaM-IQ}} \quad (4)$$

where h is the Hill coefficient. A value for h greater than one suggests the fluorescence change arose from a more complex equilibrium than just one peptide binding per calmodulin.

To carry out stoichiometric-titration experiments (calmodulin concentration greater than the K_d), we used a low concentration of Alexa-calmodulin as a reporter and added an excess of unlabeled calmodulin. For simplicity in analysis, we assumed that Alexa-calmodulin behaved identically to calmodulin, and thus this calmodulin mixture was equivalent to a decrease in specific activity (fluorescence quench) of calmodulin. We then solved the bimolecular-binding isotherm to enable us to plot the to-

tal ligand concentration (T) added versus fluorescence intensity (I). The concentration of peptide bound (B) was:

$$B = m\,[\mathrm{CaM}]\,f_{\mathrm{CaM\text{-}IQ}} \quad (5)$$

where m is the number of binding sites per calmodulin and [CaM] is the fixed concentration of calmodulin. The free concentration of IQ peptide (F) was $T - B$. We substituted the expression for B in equations (2) and (5) into:

$$\frac{B}{m[\mathrm{CaM}]} = \frac{F}{F + \mathrm{K_d}} \quad (6)$$

Note that n [CaM] is the maximum amount of IQ peptide that can bind (B_{max}). We then solved equation (6) for fluorescence intensity using Mathematica 4.0 (Wolfram Research, Champaign, IL):

$$I = -\frac{1}{2m[\mathrm{CaM}]}\left(-\mathrm{K_d}I_{\mathrm{CaM-IQ}} - m[\mathrm{CaM}]I_{\mathrm{CaM-IQ}} - m[\mathrm{CaM}]I_{\mathrm{CaM}} - TI_{\mathrm{CaM-IQ}} + \left(I_{\mathrm{CaM-IQ}} - I_{\mathrm{CaM}}\right)\sqrt{2\mathrm{K_d} + 2m\mathrm{K_d}[\mathrm{CaM}] + m^2[\mathrm{CaM}]^2 + 2\mathrm{K_d}T - 2mT[\mathrm{CaM}] + T^2}\right) \quad (7)$$

For m = 1, the only free parameters were K_d and $I_{CaM\text{-}IQ}$. We were forced to include $I_{CaM\text{-}IQ}$ as one of the fit parameters; the limited solubility of IQ peptides in the assay solution prevented us from using very high peptide concentrations that would independently establish its value by producing a plateau in the T vs. I plot. We then used the value of $I_{CaM\text{-}IQ}$ determined from the m = 1 fit and refit the data for m = 2, using K_d as the only free parameter. To judge the stoichiometry, we compared by eye the effectiveness of the fit under the two conditions.

Baculovirus constructs

Using methods described previously for rat Myo1c [43], we cloned full-length bullfrog Myo1c into the baculovirus transfer vector pBlueBacHis2B (Invitrogen, Carlsbad, CA), introducing an N-terminal hexahistidine tag for purification and a DLYDDDDK epitope tag for antibody detection. Baculoviruses were generated, purified, and characterized using standard techniques [43,45].

Protein expression and purification

Bullfrog Myo1c or its neck-tail fragment (Fig. 1A,1B) were co-expressed with *Xenopus* calmodulin in Sf9 cells using methods described previously [43]. *Xenopus* calmodulin is identical to all other sequenced vertebrate calmodulins, including bovine calmodulin [46]; we presume that bullfrog calmodulin is also identical. Recombinant proteins were partially purified by centrifugation of an Sf9-cell extract and Ni^{2+}-nitrilotriacetic acid chromatography [43]; further purification was achieved using gel filtration at 4°C on a 25-ml Superdex 200 HR 10/30 column run at 0.5 ml/min in 400 mM KCl, 1 mM $MgCl_2$, 100 μM EGTA, 15 mM HEPES pH 7.5 with an AKTA-FPLC system (Amersham Pharmacia Biotech, Piscataway, NJ). The concentration of each purified recombinant protein was calculated by measuring absorption at 280 nm and using extinction coefficients calculated from the appropriate aminoacid sequence using the ExPASy ProtParam tool [http://www.expasy.ch/tools/protparam.html], assuming 2.5 calmodulins per full-length Myo1c (53,619 $M^{-1}cm^{-1}$) or T701 fragment (65,565 $M^{-1}cm^{-1}$). We typically obtained 100–300 μg of recombinant protein from ~10^9 Sf9 cells. Full-length Myo1c had NH_4Cl-activated ATPase activity [12] of 1.8 ± 0.7 s^{-1}, with a K_m for ATP of 0.3 ± 0.1 mM. Actin activated basal Mg^{2+}-ATPase activity ~15-fold. Calmodulin was purified from bovine brain (Pel-Freez, Rogers, AR) by isoelectric precipitation and phenyl-agarose (Sigma, St. Louis, MO) chromatography [47]; its concentration was measured assuming a molar extinction coefficient of 3030 M^{-1} cm^{-1} at 276 nm [48].

Gel filtration

Stokes radii of Myo1c and T701-Myo1c were measured using gel filtration on a 25-ml Superdex 200 HR 10/30 column at either 4°C or room temperature (23–25°C). Columns were run at 0.5 ml/min in 400 mM KCl, 1 mM $MgCl_2$, 15 mM HEPES pH 7.5, and either 100 μM EGTA or 25 μM $CaCl_2$; 5–20 μg of recombinant protein was applied to the column. Columns were calibrated using 20–200 μg each of globular proteins of known Stokes radii (thyroglobulin, 8.50 nm; ferritin, 6.10 nm; catalase, 5.22 nm; aldolase, 4.81 nm; bovine serum albumin, 3.55 nm; ovalbumin, 3.05 nm; chymotrypsinogen, 2.09 nm; and RNase A, 1.64 nm; all obtained from Amersham Pharmacia Biotech). Proteins were detected by absorption at 280 nm.

Velocity sedimentation on sucrose gradients

Sedimentation coefficients of full-length and T701-Myo1c were measured using linear 5–20% sucrose gradients in 11.5 ml of 400 mM KCl, 1 mM $MgCl_2$, 15 mM HEPES pH 7.5, 0.2 mM phenylmethylsulfonyl fluoride, 10 μM leupeptin, 10 μM pepstatin, and either 100 μM EGTA or 25 μM $CaCl_2$. Gradients were calibrated with 2–20 μg internal standards of known sedimentation coefficients (catalase, 11.3 S; bovine serum albumin, 4.31 S; lysozyme, 1.91 S; all obtained from Sigma-Aldrich). After centrifugation at 33,000–40,000 rpm in an SW 41 rotor for 15–18 hours at 4°C or 25°C, gradients were fractionated from the bottom into ~30 fractions. Calibration proteins were located using a Bradford protein assay [49]; Myo1c-containing fractions were located by ELISA [43] using an antibody against the Myo1c tail (mT2/M2; ref. [50]) or against the DLYDDDDK epitope tag (anti-Xpress; Invitrogen). To determine the location of protein peaks, plots of fraction number versus the levels of Myo1c or calibration proteins were fit with either one, two, or three Gaussian curves.

For calmodulin preloading of T701-Myo1c, 10 μM purified calmodulin was incubated with 1 μM Myo1c in a so-

lution containing either 100 μM EGTA or 25 μM $CaCl_2$ for 60 min at room temperature prior to centrifugation.

Determination of molecular mass

We used the modified Svedberg equation for molecular-mass determination:

$$M = \frac{6\pi\eta Nas}{1 - \bar{v}\rho} \quad (8)$$

where M = molecular mass, η = viscosity of the medium, N = Avogadro's number, a = Stokes radius, s = sedimentation coefficient, $\bar{v}$ = partial specific volume, and ρ = density of the medium. Partial specific volume was calculated from the composition of Myo1c or T701-Myo1c, along with the appropriate number of calmodulins, by summing the partial specific volumes of each amino acid [30]. We used $\eta = 1.002 \times 10^{-2}$ g cm^{-1} s^{-1} and $\rho = 0.998$ g cm^{-3}.

Errors in molecular mass were propagated from standard deviations for Stokes radius and sedimentation coefficient measurements. To calculate error in calmodulin stoichiometry, we used the conservative assumption that all error in the molecular-mass measurement was due to variability in the number of calmodulins.

The frictional ratio was determined from:

$$\frac{f}{f_0} = \left(\frac{a}{3\bar{v}M/4\pi N} \right)^{1/3} \quad (9)$$

where f is the frictional coefficient of the Myo1c-calmodulin complex and f_0 is the frictional coefficient of a sphere of equal volume. Accordingly, the frictional ratio of a globular protein will be 1; that of an elongated protein will be >1.

Stoichiometry determination by gel scanning

T701-Myo1c and bovine-brain calmodulin were separated by sodium dodecyl sulfate gel electrophoresis (SDS-PAGE) and stained with Coomassie blue R250. Gels were scanned with a flatbed scanner; calmodulin was quantified using analysis of the resulting images with NIH Image version 1.62. The concentration of the T701-Myo1c heavy chain was determined by measuring absorbance at 280 nm, although the analysis was complicated by the uncertain calmodulin stoichiometry (p). To circumvent this problem, we solved several simultaneous equations for p. The molar extinction coefficient of the T701-Myo1c/calmodulin complex ($\epsilon_{T701\text{-}CaM}$) is given by:

$$\epsilon_{T701\text{-}CaM} = \epsilon_{T701} + p \cdot \epsilon_{CaM} \quad (10)$$

where ϵ_{T701} is the extinction coefficient of the T701-Myo1c heavy chain alone (57,990 M^{-1} cm^{-1}), ϵ_{CaM} is the extinction coefficient of calmodulin (2560 M^{-1}cm^{-1}), and p is the calmodulin:T701 stoichiometry. The concentration of T701-Myo1c heavy chain is given by:

$$[T701_{HC}] = \frac{A280}{\varepsilon_{T701\text{-}CaM}} \quad (11)$$

where A280 is the absorbance of the complex at 280 nm for a 1 cm pathlength. Finally,

$$p \cdot [T701_{HC}] = [CaM] \quad (12)$$

where [CaM] is the calmodulin concentration determined by gel scanning. Solving for p:

$$p = \frac{[CaM] \cdot \varepsilon_{T701}}{A280 - [CaM] \cdot \varepsilon_{CaM}} \quad (13)$$

Other methods

We measured the free Ca^{2+} concentrations in our solutions using spectrofluorometry with Calcium Green-2 (Molecular Probes). SDS-PAGE was carried out with 18% acrylamide Criterion gels (Bio-Rad Laboratories; Hercules, CA); gels were stained with Coomassie blue R250.

Authors' contributions

Author 1 (PGG) conceived of the experimental approach, carried out many of the experiments, supervised the technician who performed the remainder, developed the methods for analysis, analyzed and interpreted the data, and wrote the manuscript. Author 2 (JLC) contributed to the development of the experimental approach, helped analyze and interpret the data, and edited the manuscript.

Acknowledgements

We thank Dr. Serge Jean for producing the original full-length bullfrog Myo1c baculovirus construct. Weiyi Zhao provided excellent technical support; Drs. Susan Gillespie and Kevin Nusser provided additional support and advice. Research was supported by NIH grant DC02368.

References

1. Gillespie PG, Albanesi JP, Bahler M, Bement WM, Berg JS, Burgess DR, Burnside B, Cheney RE, Corey DP, Coudrier E, de Lanerolle P, Hammer JA, Hasson T, Holt JR, Hudspeth AJ, Ikebe M, Kendrick-Jones J, Korn ED, Li R, Mercer JA, Milligan RA, Mooseker MS, Ostap EM, Petit C, Pollard TD, Sellers JR, Soldati T, Titus MA: **Myosin-I nomenclature.** *J Cell Biol* 2001, **155:**703-704
2. Pestic-Dragovich L, Stojiljkovic L, Philimonenko AA, Nowak G, Ke Y, Settlage RE, Shabanowitz J, Hunt DF, Hozak P, de Lanerolle P: **A myosin I isoform in the nucleus.** *Science* 2000, **290:**337-341
3. Wang FS, Wolenski JS, Cheney RE, Mooseker MS, Jay DG: **Function of myosin-V in filopodial extension of neuronal growth cones.** *Science* 1996, **273:**660-663
4. Diefenbach TJ, Latham VM, Yimlamai D, Liu CA, Herman IM, Jay DG: **Myosin 1c and myosin IIB serve opposing roles in lamellipodial dynamics of the neuronal growth cone.** *J Cell Biol* 2002, **158:**1207-1217
5. Boyd-White J, Srirangam A, Goheen MP, Wagner MC: **Ischemia disrupts myosin Ibeta in renal tubules.** *Am J Physiol Cell Physiol* 2001, **281:**C1326-1335
6. Wagner MC, Molitoris BA: **ATP depletion alters myosin Iβ cellular location in LLC-PK1 cells.** *Am J Physiol* 1997, **272:**C1680-1690

7. Holt JR, Gillespie SK, Provance DW, Shah K, Shokat KM, Corey DP, Mercer JA, Gillespie PG: **A chemical-genetic strategy implicates myosin-1c in adaptation by hair cells.** *Cell* 2002, **108:**371-381
8. Berg JS, Powell BC, Cheney RE: **A millennial myosin census.** *Mol Biol Cell* 2001, **12:**780-794
9. Dumont RD, Zhao Y-d, Holt JR, Bähler M, Gillespie PG: **Myosin-I isozymes in neonatal rodent auditory and vestibular epithelia.** *J Assoc Res Otolaryngol* 2002
10. Solc CK, Derfler BH, Duyk GM, Corey DP: **Molecular cloning of myosins from bullfrog saccular macula: a candidate for the hair cell adaptation motor.** *Auditory Neurosci* 1994, **1:**63-75
11. Sokac AM, Bement WM: **Regulation and expression of metazoan unconventional myosins.** *Int Rev Cytol* 2000, **200:**197-304
12. Barylko B, Wagner MC, Reizes O, Albanesi JP: **Purification and characterization of a mammalian myosin I.** *Proc Natl Acad Sci U S A* 1992, **89:**490-494
13. Cyr JL, Dumont RA, Gillespie PG: **Myosin-1c interacts with hair-cell receptors through its calmodulin-binding IQ domains.** *J Neurosci* 2002, **22:**2487-2495
14. Rhoads AR, Friedberg F: **Sequence motifs for calmodulin recognition.** *Faseb J* 1997, **11:**331-340
15. Reizes O, Barylko B, Li C, Südhof TC, Albanesi JP: **Domain structure of a mammalian myosin I.** *Proc Natl Acad Sci U S A* 1994, **91:**6349-6353
16. Sherr EH, Joyce MP, Greene LA: **Mammalian myosin Iα, Iβ, and Iγ: new widely expressed genes of the myosin I family.** *J Cell Biol* 1993, **120:**1405-1416
17. Ruppert C, Godel J, Muller RT, Kroschewski R, Reinhard J, Bähler M: **Localization of the rat myosin I molecules myr 1 and myr 2 and in vivo targeting of their tail domains.** *J Cell Sci* 1995, **108:**3775-3786
18. Metcalf AB, Chelliah Y, Hudspeth AJ: **Molecular cloning of a myosin Iβ isozyme that may mediate adaptation by hair cells of the bullfrog's internal ear.** *Proc Natl Acad Sci U S A* 1994, **91:**11821-11825
19. Zhu T, Sata M, Ikebe M: **Functional expression of mammalian myosin I beta: analysis of its motor activity.** *Biochemistry* 1996, **35:**513-522
20. Coluccio LM: **Differential calmodulin binding to three myosin-I isoforms from liver.** *J Cell Sci* 1994, **107:**2279-2284
21. Chacko S, Jacob SS, Horiuchi KY: **Myosin I from mammalian smooth muscle is regulated by caldesmon-calmodulin.** *J Biol Chem* 1994, **269:**15803-15807
22. Rayment I, Rypniewski RW, Schmidt-Base K, Smith R, Tomchick DR, Benning MM, Winkelmann DA, Wessenberg G, Holden HM: **Three-dimensional structure of myosin subfragment-1: a molecular motor.** *Science* 1993, **261:**50-58
23. Uyeda TQ, Abramson PD, Spudich JA: **The neck region of the myosin motor domain acts as a lever arm to generate movement.** *Proc Natl Acad Sci U S A* 1996, **93:**4459-4464
24. Chapman ER, Au D, Alexander KA, Nicolson TA, Storm DR: **Characterization of the calmodulin binding domain of neuromodulin. Functional significance of serine 41 and phenylalanine 42.** *J Biol Chem* 1991, **266:**207-213
25. Alexander KA, Cimler BM, Meier KE, Storm DR: **Regulation of calmodulin binding to P-57. A neurospecific calmodulin binding protein.** *J Biol Chem* 1987, **262:**6108-6113
26. Lumpkin EA, Hudspeth AJ: **Regulation of free Ca^{2+} concentration in hair-cell stereocilia.** *J Neurosci* 1998, **18:**6300-6318
27. Panchuk-Voloshina N, Haugland RP, Bishop-Stewart J, Bhalgat MK, Millard PJ, Mao F, Leung WY: **Alexa dyes, a series of new fluorescent dyes that yield exceptionally bright, photostable conjugates.** *J Histochem Cytochem* 1999, **47:**1179-1188
28. Jurado LA, Chockalingam PS, Jarrett HW: **Apocalmodulin.** *Physiol Rev* 1999, **79:**661-682
29. Siegel LM, Monty KJ: **Determination of molecular weights and frictional ratios of proteins in impure systems by use of gel filtration and density gradient centrifugation. Application to crude preparations of sulfite and hydroxylamine reductases.** *Biochim Biophys Acta* 1966, **112:**346-362
30. Prakash V, Timasheff SN: **Calculation of partial specific volumes of proteins in 8 M urea solution.** *Methods Enzymol* 1985, **117:**3-60
31. Olwin BB, Storm DR: **Preparation of fluorescent labeled calmodulins.** *Methods Enzymol* 1983, **102:**148-157
32. Houdusse A, Silver M, Cohen C: **A model of Ca^{2+}-free calmodulin binding to unconventional myosins reveals how calmodulin acts as a regulatory switch.** *Structure* 1996, **4:**1475-1490
33. Walker RG, Hudspeth AJ, Gillespie PG: **Calmodulin and calmodulin-binding proteins in hair bundles.** *Proc Natl Acad Sci U S A* 1993, **90:**2807-2811
34. Kakiuchi S, Yasuda S, Yamazaki R, Teshima Y, Kanda K, Kakiuchi R, Sobue K: **Quantitative determinations of calmodulin in the supernatant and particulate fractions of mammalian tissues.** *J Biochem (Tokyo)* 1982, **92:**1041-1048
35. Mooseker MS: **Organization, chemistry, and assembly of the cytoskeletal apparatus of the intestinal brush border.** *Annu Rev Cell Biol* 1985, **1:**209-241
36. Rivas G, Stafford W, Minton AP: **Characterization of heterologous protein-protein interactions using analytical ultracentrifugation.** *Methods* 1999, **19:**194-212
37. Cann JR, Coombs RO, Howlett GJ, Jacobsen MP, Winzor DJ: **Effects of molecular crowding on protein self-association: a potential source of error in sedimentation coefficients obtained by zonal ultracentrifugation in a sucrose gradient.** *Biochemistry* 1994, **33:**10185-10190
38. Zhu T, Beckingham K, Ikebe M: **High affinity Ca^{2+} binding sites of calmodulin are critical for the regulation of myosin Iβ motor function.** *J Biol Chem* 1998, **273:**20481-20486
39. Gillespie PG, Corey DP: **Myosin and adaptation by hair cells.** *Neuron* 1997, **19:**955-958
40. Howard J, Spudich JA: **Is the lever arm of myosin a molecular elastic element?** *Proc Natl Acad Sci U S A* 1996, **93:**4462-4464
41. Espindola FS, Suter DM, Partata LB, Cao T, Wolenski JS, Cheney RE, King SM, Mooseker MS: **The light chain composition of chicken brain myosin-Va: calmodulin, myosin-II essential light chains, and 8-kDa dynein light chain/PIN.** *Cell Motil Cytoskeleton* 2000, **47:**269-281
42. Rogers MS, Strehler EE: **The tumor-sensitive calmodulin-like protein is a specific light chain of human unconventional myosin X.** *J Biol Chem* 2001, **276:**12182-12189
43. Gillespie PG, Gillespie SK, Mercer JA, Shah K, Shokat KM: **Engineering of the myosin-Iβ nucleotide-binding pocket to create selective sensitivity to N^6-modified ADP analogs.** *J Biol Chem* 1999, **274:**31373-31381
44. Mann D, Vanaman TC: **Specific chemical modification as a probe of calmodulin function.** *Methods Enzymol* 1987, **139:**417-433
45. O'Reilly DR, Miller LK, Luckow VA: **Baculovirus Expression Vectors:** *A Laboratory Manual New York: Oxford University Press* 1994
46. Toutenhoofd SL, Strehler EE: **The calmodulin multigene family as a unique case of genetic redundancy: multiple levels of regulation to provide spatial and temporal control of calmodulin pools?** *Cell Calcium* 2000, **28:**83-96
47. Gopalakrishna R, Anderson WB: **Ca^{2+}-induced hydrophobic site on calmodulin: application for purification of calmodulin by phenyl-Sepharose affinity chromatography.** *Biochem Biophys Res Commun* 1982, **104:**830-836
48. Wallace RW, Tallant EA, Cheung WY: **Assay of calmodulin by Ca^{2+}-dependent phosphodiesterase.** *Methods Enzymol* 1983, **102:**39-47
49. Bradford MM: **A rapid and sensitive method for the quantitation of microgram quantities of protein utilizing the principle of protein-dye binding.** *Anal Biochem* 1976, **72:**248-254
50. Wagner MC, Barylko B, Albanesi JP: **Tissue distribution and subcellular localization of mammalian myosin I.** *J Cell Biol* 1992, **119:**163-170